Rapid Preparation of Branched and Degradable AIE-active Fluorescent Organic Nanoparticles via Formation of Dynamic Phenyl Borate Bond

Zi Long[a,#], Meiying Liu[a,#], Liucheng Mao[a], Guangjian Zeng[a], Qing Wan[a], Dazhuang Xu[a], Fengjie Deng[a,*], Hongye Huang[a], Xiaoyong Zhang[a,*], Yen Wei[b,*]

a College of Chemistry, Nanchang University, 999 Xuefu Avenue, Nanchang 330031, China.

b Department of Chemistry and the Tsinghua Center for Frontier Polymer Research, Tsinghua University, Beijing, 100084, China.

# These authors contributed equally to this work

Fengjie Deng, Tel. +86-791-8396-9553
Email: fengjiedeng@aliyun.com

Xiaoyong Zhang, Tel. +86-791-8396-9553
Email: Xiaoyongzhang1980@gmail.com

Yen Wei, Tel. +86-10-6277-2674; Fax: +86-10-6277-1149
Email: weiyen@tsinghua.edu.cn

Abstract

The fluorescent organic nanoparticles (FNPs) with aggregation-induced emission (AIE) feature have received increasing attention for their advanced optical properties. Although many efforts have been devoted to the fabrication and biomedical applications of AIE-active FNPs, the preparation of branched AIE-active FNPs with degradability through formation of dynamic bonds have rarely been reported. In this work, branched AIE-active FNPs were fabricated via dynamic linkage of hydrophobic hyperbranched and degradable Boltorn H40 (H40) with phenylboronic acid terminated AIE dye ($PhB(OH)_2$) and mPEG ($mPEG\text{-}B(OH)_2$), which relied on a facile one-pot strategy between phenylboronic acid and diol group of H40. The branched H40-star-mPEG-$PhB(OH)_2$ FNPs were characterized using nuclear magnetic resonance spectroscopy, Fourier transform infrared spectroscopy, and fluorescence spectroscopy. Benefiting from their highly branched structure and amphiphilic properties, H40-star-mPEG-$PhB(OH)_2$ could self-assemble into micelles and emit strong orange-red fluorescence. More importantly, cell viability results demonstrated that H40-star-mPEG-$PhB(OH)_2$ FNPs showed good biocompatibility and promising candidates for bio-imaging. Taken together, we developed a one-pot strategy for preparation of branched AIE-active FNPs through the formation of dynamic phenyl borate. The resultant H40-star-mPEG-$PhB(OH)_2$ FNPs should be promising biomaterials for different applications for biodegradability of H40 and responsiveness of phenyl borate.

Key words: Aggregation-induced emission, branched polymers, biodegradable, dynamic bonds, responsiveness

1. Introduction

Fluorescence techniques are powerful tools for bio-imaging, which allow direct visualization of biological analytes at the molecular level and offer useful insights into complex biological structures and processes since fluorescence imaging techniques have made significant contribution to advance our knowledge in life science.[1-4] Compared with traditional positron emission tomography and magnetic resonance imaging methods, fluorescence imaging techniques give unique advantages such as high sensitivity, spatial and temporal detection abilities.[5-7] Based on development of fluorescence imaging techniques, a large number of fluorescent probes have been developed because of their high sensitivity, fast response, and excellent spatial and temporal resolution.[8-11] Fluorescent inorganic nanoparticles (FINs), such as quantum dots (QDs), luminescent metal nanoclusters, and Ln ions doped materials are highly luminescent and resistant to photobleaching, but most of them are poor degradable and toxic to living organisms.[12-15] As compared with FINs, fluorescent organic nanoparticles (FNPs) have good biocompatibility, well designability and biodegradability, which making them promising alternatives for biological imaging applications.[16-20] However, FNPs are mainly relied on the self-assembly of amphiphilic organic dyes contained copolymers, which are readily to form core shell soft nanostructures when they dispersed in aqueous solution. In these self-assemblies, the hydrophobic dyes are prone to aggregate in the core and shows obviously decrease their fluorescence intensity because of the renowned aggregation-caused quenching (ACQ) effect. Therefore, fabrication of FNPs with desirable optical properties especially strong luminescence is still challenge by using conventional organic dyes.

Thanks to the aggregation-induced emission (AIE), a unique phenomenon that exactly opposite to the ACQ effect, which was first discovered by Tang's group in 2001.[21] Different from the conventional organic dyes, the dyes with AIE feature were emitted much enhanced fluorescence in their aggregation state. The restriction of intramolecular rotations (RIR) that prohibited energy dissipation via non-radiative channels has been regarded as one of the AIE mechanism.[22-25] These advantages made AIE luminogens particularly attractive for biological applications.[26-33] Based on the concept of AIE, a powerful and versatile strategy has been developed for designing fluorescent probes,[34-37] chem-sensors [38-41] and optical materials.[42-45] Over the past few years, a large number of AIE-active FNPs have been fabricated via different strategies, however, fabrication of degradable AIE-active FNPs has rarely been reported.[46] To date, no studies have reported the

fabrication of branched AIE-active FNPs via the formation of dynamic bonds.

Phenyl borate is a dynamic bond, which can response to both pH and glucose. In this contribution, we report for the first time that novel branched and degradable FNPs based on AIE-active dyes can be facilely fabricated via the formation of dynamic phenyl borate between Boltorn H40 (H40), boronic acid terminated methoxypolyethylene glycols (mPEG-B$(OH)_2$) and boronic acid functionalized AIE dye (PhB$(OH)_2$) (**Scheme 1**). It is well known that H40 is dendrimer-like aliphatic polyester with a large number of terminal functional hydroxyl groups (64 × OH) and has been extensively utilized as macromolecular building block to fabricate nanostructure for biomedical applications because of its good biodegradability, biocompatibility, globular architectures and chained functionalities.[47-49] Benefiting from its hydrophobic structure, the resultant star FNPs were able to self-assemble into stable micelles with emitting strong orange-red fluorescence in aqueous solution. Moreover, the self-assembled luminescent micelles showed unique characteristics such as nanosize, high-stability, and branched core-shell architecture. Besides, they exhibited good water dispersibility, biodegradability, biocompatibility and AIE property, making them extremely promising candidates for various biomedical applications including bio-imaging. Furthermore, it has been demonstrated that when hydrophobic segments are introduced at the microgels or nanogels, they could also load hydrophobic drugs.[50-55] The amphiphilic dendrimer H40-star-mPEG-PhB$(OH)_2$ FNPs consisted an aliphatic biodegradable polyester H40 inner core could also been served as the reservoir for massive hydrophobic drugs since hyperbranched, high loading capacity; while the hydrophilic mPEG outer shell enhanced the micelle stability and prolonged the circulation time in bloodstream. As compared with FNPs based on typical organic dyes, dyes with AIE feature allow the use of highly concentrated fluorogens for biological imaging, which making facile fabrication of ultrabright FNPs possible.

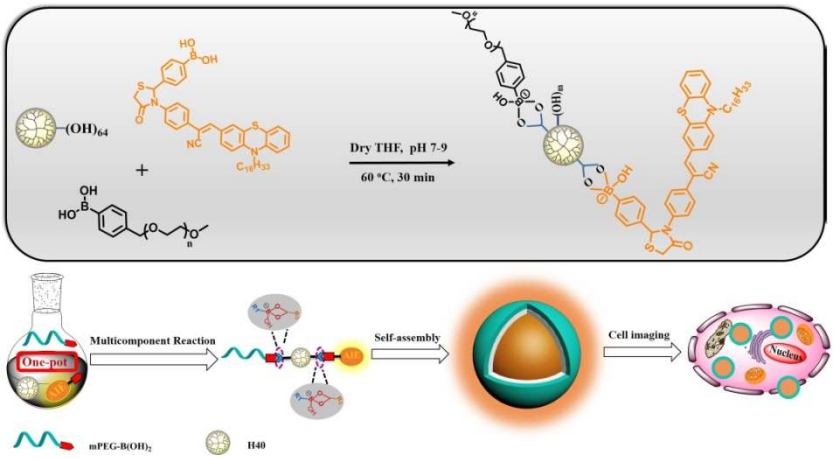

Scheme 1 Schematic showing the preparation of H40-star-mPEG-PhB(OH)$_2$ FNPs and cell imaging applications of thus obtained FNPs.

2. Experimental

2.1 Materials and methods

Hyperbranched aliphatic polyester Boltorn H40 was obtained from Seebio Biotech，Inc. Shanghai, china. 4-(bromomethyl)phenylboronic acid, 4-Formylphenylboronic acid, Phenothiazine, sodium hydride,1-Bromohexadecane, N,N-dimethylformamide, phosphoryl chloride, 4-aminobenzyl cyanide, tetrabutylammonium hydroxide (TBAH, 0.8 M in methanol), anhydrous tetrahydrofuran (THF), Dichloromethane (DCM), sodium hydride, Methoxypolyethylene glycols (M*W* = 1900 Da), Mercapto acetic acid were all purchased from Aladdin company (Shanghai, China). All chemicals were of analytical grade and were used as received without any further purification.

The chemical compositions of samples were characterized by ^{1}H nuclear magnetic resonance (NMR) spectroscopy on Bruker Avance-400 spectrometer using D_2O and $CDCl_3$ as solvents. The chemical structure information of synthetic polymers and materials were characterized by Fourier transform infrared (FT-IR) spectroscopy using KBr pellets. FT-IR spectra were supplied from Nicolet5700 (Thermo Nicolet corporation). Transmission electron microscopy (TEM) was used to characterize the size and morphology of samples. TEM images were recorded on a Hitachi 7650B microscope operated at 80 kV. The TEM specimens were got by putting a drop of the nanoparticle ethanol suspension on a carbon-coated copper grid. The fluorescence data was obtained from the Fluorescence spectrophotometer (FSP, model: C11367-11), which purchased from Hamamatsu (Japanese).

2.2 Preparation of PhB(OH)$_2$

The PhB(OH)$_2$ was synthesized via a facile and atom-economical one-pot method based on the phenothiazine derivatives (**Scheme S1**).[56] As shown in **Scheme S2**. Typically, PhNH$_2$ (28 mg, 0.050 mmol) was synthesized according to the former report.[57] 4-Formylphenylboronic acid (11 mg, 0.075 mmol) was charged into a dry Schlenk tube along with 20 mL anhydrous THF solution. The Schlenk tube was put into thermo-shaker at room temperature (25 °C) for 10 h. Then mercaptoacetic acid (69 mg, 0.75 mmol) was added into the Schlenk tube and reacted for next 8 h. The mixture was simply purified by precipitation into cold ethyl ether and washed for 3 times, dried at vacuum. ^{1}H NMR (400 MHz, $CDCl_3$, TMS, δ in ppm): δ 8.27 (m, 2H), δ 8.00 (m, 2H), δ 7.98 (s, H), δ 7.96-7.70 (m, 11H), δ

7.25 ppm (s, H), δ 3.60 (s, 2H), δ 3.0-2.97 (s, 2H), δ 2.89 ppm (m, 2H), δ 2.0 (m, 2H), δ 1.24 ppm (m, 26H), δ 0.96 (m, 3H).

2.3 Preparation of mPEG-B(OH)$_2$

mPEG with 4-(bromomethyl)phenylboronic acid end-group (mPEG-B(OH)$_2$) was synthesized according to previous report.[58] As shown in **Scheme S3**, sodium hydride (0.23 g, 5.55 mmol) was added into a solution of mPEG (3.25 g, 1.7 mmol) in 30 mL of anhydrous THF in a single portion. The resulting solution was stirred under N_2 atmosphere at room temperature for 2 h, then 4-(bromomethyl)phenylboronic acid (0.36 g, 1.7 mmol) was added in a single portion. The solution was stirred for an additional 12 h and then quenched with 11 mL of 1M HCl. After filtration, the solvents were removed using a rotary evaporator. The raw product was dissolved with DCM, Insolubles were filtered off. Then the filtrate was concentrated again and the desired product was purified by recrystallization three times in ethyl ether, and dried under vacuum at 45 °C. (2.1 g, yield: 60%). ^{1}H NMR (400 MHz, D_2O, TMS, δ in ppm): δ 7.70-6.80 (m, 4H), δ 4.60 (s, 2H), δ 4.30 (s, 2H), δ 3.70 (m, 2H), δ 3.50 ppm (m, 2H), δ 3.40 (s, 3H).

2.4 Fabrication of H40-star-mPEG-PhB(OH)$_2$ FNPs

The H40-star-mPEG-PhB(OH)$_2$ FNPs were prepared via a simple and atom-economical one-pot strategy to form dynamic phenyl borate. As shown in **Scheme 1**, H40 (200 mg), PhB(OH)$_2$ (0.09 mmol, 40 mg) were dissolved in 40 mL dry THF. Next, drops of triethylamine solution were added into reaction system at room temperature for adjusting the pH values to 7-9. Then mPEG-B(OH)$_2$ (0.20 mmol, 400 mg) was added and stirred for an another 30 min. The crude product was added dropwise into 100 mL saturated brine and extracted with ethyl acetate for 3 times. The organic layer was evaporated under vacuum. Product was purified by recrystallization in ethyl ether, and dried under vacuum at 45 °C.

2.5 Cytotoxicity evaluation of H40-star-mPEG-PhB(OH)$_2$ FNPs

The effect of H40-star-mPEG-PhB(OH)$_2$ FNPs on the metabolic activity of HeLa cells was assessed by a typical Cell Counting Kit-8 (CCK-8) assay.[59-61] The HeLa cells were seeded in a 96-well plate with the density of 5×10^4 cells per well and incubated at 37 °C for 24 h. Then the samples with a series of predetermined concentrations were prepared and added into the experimental wells for 12 and 24 h, respectively. Then the nanoparticles were removed and the cells were washed with phosphate buffer solution (PBS) three times. 10 μL of CCK-8 dye and 100 μL of Dulbecco's Modified Eagle's medium

(DMEM) were added to each well and incubated for another 2 h at 37 °C. The plates were shaken for 10 min, and the absorbance was measured by microplate reader (Victor III, Perkin-Elmer) at 450 nm. The percentage of cell viability was calculated relative to negative control (media alone). Three replicates were performed for each sample and the mean values were used as the final data.

2.6 Biological imaging of cells using H40-star-mPEG-PhB(OH)$_2$ FNPs

Biological imaging of HeLa cells using H40-star-mPEG-PhB(OH)$_2$ FNPs were conducted with a confocal laser scanning microscopy (CLSM) Zeiss 710 3-channel (Zeiss, Germany), with the excitation wavelength was set as 458 nm. HeLa cells were cultivated in Dulbecco's modified eagle medium (DMEM) supplemented with 10% heat-inactivated fetal bovine serum (FBS), 2 mM glutamine, 100 U mL^{-1} penicillin, and 100 μg mL^{-1} of streptomycin. Cell culture was kept at 37 °C under a wet condition with 95% air, 5% CO_2 in culture medium. Culture medium was altered every three days to maintain the exponential growth of the cells. On the day before treatment, cells were seeded in a glass bottom dish with a density of 1×10^5 cells per dish. On the day of treatment, the cells were incubated with H40-star-mPEG-PhB(OH)$_2$ FNPs with an eventual concentration of 40 μg mL^{-1} for 3 h at 37°C. Later, the cells were washed three times with PBS to remove the H40-star-mPEG-PhB(OH)$_2$ FNPs then fixed with 4 % paraformaldehyde for 10 min at room temperature.

3. Results and discussion

3.1 Characterization of H40-star-mPEG-PhB(OH)$_2$ FNPs

As the hydrophobic AIE dye reacted with hydrophobic H40 via introducing the hydrophilic mPEG-B(OH)$_2$ by a ‘one pot’ method, the amphipathic H40-star-mPEG-PhB(OH)$_2$ FNPs were prepared. These AIE-active FNPs emitted strong orange-red fluorescence in aqueous solution with excellent water dispersibility and cytocompability. To confirm the successful conjugation of H40 with mPEG-B(OH)$_2$, PhB(OH)$_2$, the structures of H40, mPEG-B(OH)$_2$ and H40-star-mPEG-PhB(OH)$_2$ were determined by ^{1}H NMR analysis in D_2O (**Fig. 1**). As displayed in **Fig. 1**, compared with ^{1}H NMR curves of H40, mPEG-B(OH)$_2$, some peaks appeared at 6.5-7.5 ppm, which could be ascribed to benzene ring, and a chemical shift around 0.08 ppm was clearly observed according to mPEG-B(OH)$_2$. The peaks located at 1.1 and 4.2 ppm were belonged to –CH_2-OH of H40. Moreover, compared with H40, the intensity of the two peaks was reduced significantly, indicating that most of hydroxyl groups were reacted with the B(OH)$_2$ of mPEG-B(OH)$_2$ and PhB(OH)$_2$. It further demonstrated that the diol

group of H40 could react with phenylboronic acid via dehydration cyclization and formed stable cyclic borate esters. Besides, the peaks of -CH_2-CH_2-O group around 3.6 ppm in H40-star-mPEG-PhB$(OH)_2$ could be assigned to the mPEG-B$(OH)_2$, while the peaks of –S-CH_2-C(O) appeared could be ascribed to the introduction of PhB$(OH)_2$. All of the ^{1}H NMR results confirmed the successful formation of H40-star-mPEG-PhB$(OH)_2$ FNPs through formation of dynamic phenyl borate between the diol group of H40 and phenylboronic acid group of mPEG and AIE dye.

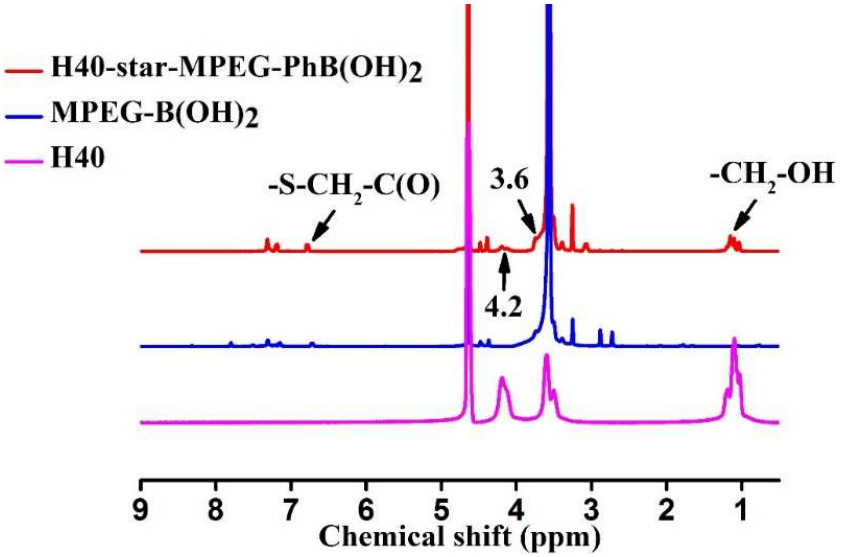

Fig. 1 ^{1}H NMR spectrum of H40-star-mPEG-PhB$(OH)_2$, mPEG-B$(OH)_2$, H40 in $CDCl_3$.

The molecular structure of H40-star-mPEG-PhB$(OH)_2$ was further verified by FT-IR spectra. As shown in **Fig. 2**, the stretching vibration of the -CH_2 group was observed at 2820 cm^{-1}, the strong peak at 1111 cm^{-1} was assigned to the C-O-C stretching vibration of ether in mPEG backbone, indicating the presence of mPEG-B$(OH)_2$. Meanwhile, a series of peaks distributed from 1560 to 1450 cm^{-1} could be ascribed to the stretching vibration of aromatic rings. Peaks at 1700 cm^{-1} in H40-star-mPEG-PhB$(OH)_2$ were caused by the stretching vibration of ester of H40, proving the presence of H40. Moreover, after H40 covalent binding with PhB$(OH)_2$, the –N-C=O stretching vibration peak that belonged to PhB$(OH)_2$ was shifted from 1568 to 1634 cm^{-1}, demonstrating PhB$(OH)_2$ existed in H40-star-mPEG-PhB$(OH)_2$. Besides, a new peak appeared at 1508 cm^{-1} can be attributed to the cyclic boron esters (-B-O). All the above results confirmed the formation of H40-star-mPEG-PhB$(OH)_2$.

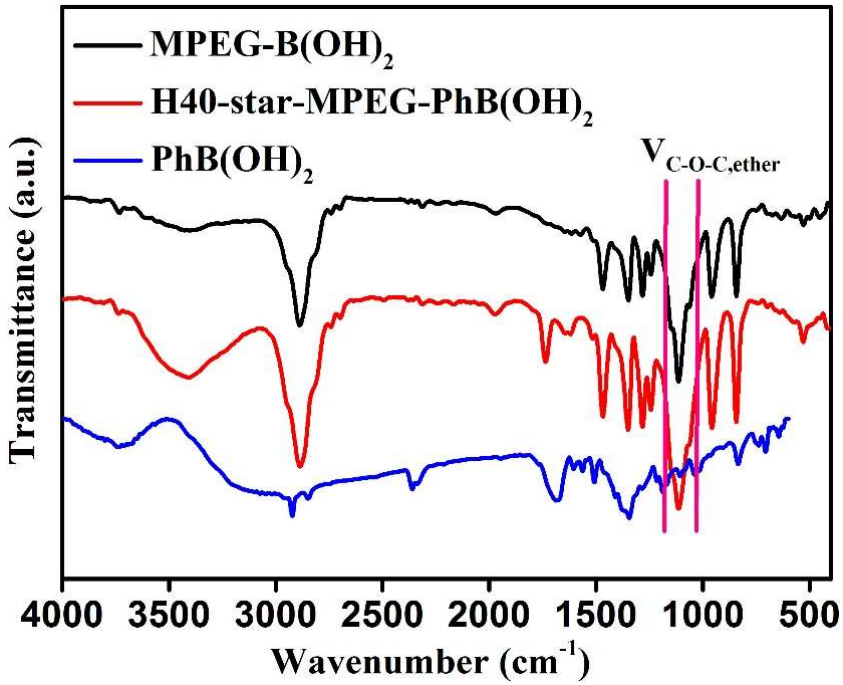

Fig. 2 FT-IR spectra of mPEG-B(OH)$_2$, H40-star-mPEG-PhB(OH)$_2$ and PhB(OH)$_2$. Many characteristic peaks were appeared in the sample of H40-star-mPEG-PhB(OH)$_2$ as compared with PhB(OH)$_2$. These peaks were located at 2920 and 1111 cm^{-1}, respectively.

The amphiphilic H40-star-mPEG-PhB(OH)$_2$ FNPs were apt to self-assemble and form nanoparticles with strong orange-red fluorescence when they were dispersed in aqueous solution, which made their promising for various biomedical applications. As a result, TEM characterization was carried out to determine the size and morphology. As presented in **Fig. 3**, H40-star-mPEG-PhB(OH)$_2$ FNPs exhibited a relative uniform spherical shape with an average diameter of a few hundred nanometers, proving thus synthetic amphiphilic AIE-active polymeric materials are formed by self-assembly. More importantly, because hydrophilic mPEG-B(OH)$_2$ was covered on hydrophobic H40, the final H40-star-mPEG-PhB(OH)$_2$ FNPs show great dispersibility in aqueous solution, while the hydrophobic H40 and AIE dye were encapsulated in the core of FNPs, resulting in enhanced fluorescence. More importantly, the responsibility of H40-star-mPEG-PhB(OH)$_2$ FNPs towards glucose and pH was also investigated. As shown in **Fig. S2**, the water suspension H40-star-mPEG-PhB(OH)$_2$ FNPs have not changed after 5 mmol/L glucose were added. It is likely due to the formation of glucose-mPEG-PhB(OH)$_2$ complex. However, when the pH value was adjusted to 5.5, these H40-star-mPEG-PhB(OH)$_2$ FNPs were quickly aggregated.

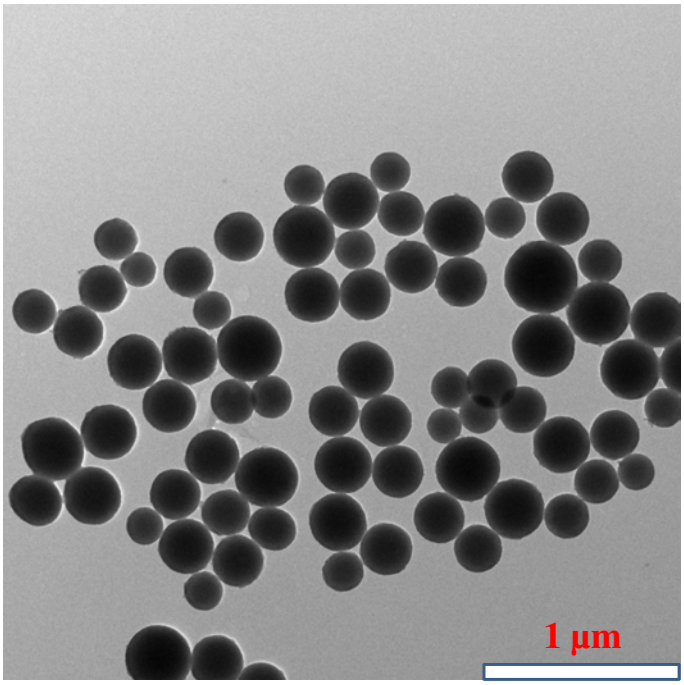

Fig. 3 TEM image of H40-star-mPEG-PhB(OH)$_2$ FNPs dispersed in water. Many spherical nanoparticles with diameter of a few hundred nanometers were found by TEM images. The results clearly evidenced that these amphiphilic copolymers were self-assembled in aqueous solution.

The optical properties of H40-star-mPEG-PhB(OH)$_2$ FNPs were determined by UV-Vis absorption spectroscopy and fluorescence spectroscopy. As shown in **Fig. 4A**, it showed that H40-star-mPEG-PhB(OH)$_2$ FNPs possessed multiple absorption peaks. The adsorption peak at 204 nm was attributed to the π→π* transition of C=C of aromatic rings. While the other adsorption peak located at 270 nm was assigned as n→π* transition of -C=O and –C≡N. Besides, a long band edge lift could be observed from water suspension of H40-star-mPEG-PhB(OH)$_2$ FNPs, indicating that AIE-active FNPs were formed according to the Mie scattering theory. The UV-Vis spectra evidenced that H40-star-mPEG-PhB(OH)$_2$ FNPs were indeed formed because H40 and mPEG were absent of adsorption in these regions. Furthermore, we also observed that H40-star-mPEG-PhB(OH)$_2$ FNPs could be well dispersed in pure aqueous solution. As shown in inset of **Fig. 4A**, the logo of "AIE" as background can be observed when H40-star-mPEG-PhB(OH)$_2$ FNPs was in water dispersion. As the introduction of the AIE fluorogen (PhB(OH)$_2$) for the FNPs, H40-star-mPEG-PhB(OH)$_2$ also emitted strong orange-red fluorescence in water. The fluorescent spectra of H40-star-mPEG-PhB(OH)$_2$ in water was implemented to quantitatively confirm their excitation and emission wavelengths. As shown in **Fig.**

4B, the maximum emission wavelength of H40-star-mPEG-PhB(OH)$_2$ FNPs was located at 577 nm, while their maximum excitation wavelength was located at 447 nm. Well consistent with the fluorescent spectra, orange-red fluorescence was observed after the water suspension of H40-star-mPEG-PhB(OH)$_2$ FNPs were irradiated by UV lamp at 365 nm (Inset of **Fig. 4B**). Moreover, we could also found that the excitation spectrum was rather broad, indicating that the H40-star-mPEG-PhB(OH)$_2$ FNPs could be excited with many types of laser with different wavelengths. Photostability is very important for the biological imaging applications of fluorescent probes. It has been demonstrated that the fluorescent nanoparticles could exhibit better optical stability as compared with small organic dyes. Herein, the optical stability of H40-star-mPEG-PhB(OH)$_2$ FNPs was examined using UV lamp irradiation. As shown in **Fig. S1**, the maximum emission fluorescent intensity value from 5653 decreased to 5328 after the water suspension of H40-star-mPEG-PhB(OH)$_2$ FNPs was continuously irradiated using UV lamp (365 nm) for 2 h, suggesting that H40-star-mPEG-PhB(OH)$_2$ FNPs possessed excellent fluorescence stability. Thus excellent photostability is very useful biological imaging especially for long-term fluorescent tracing. Furthermore, Hyperbranched polymers H40 as the hydrophobic core of thus FNPs are promising candidates for drug delivery systems because of their intrinsic features, such as branching architecture, a large number of terminal functional groups, and good solubility.[62-64]

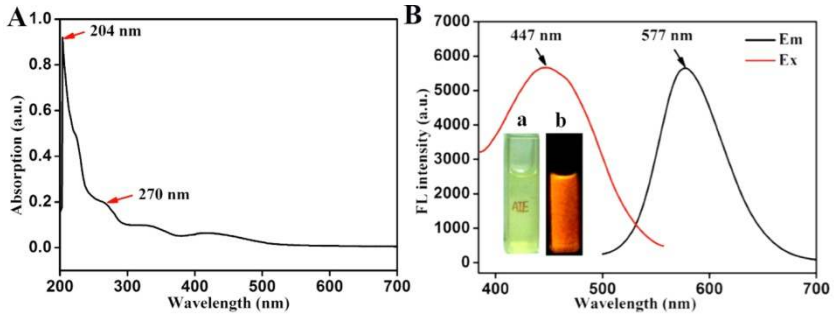

Fig. 4 (A) UV-Vis spectrum of H40-star-mPEG-PhB(OH)$_2$ FNPs. (B) fluorescence excitation (Ex) and emission (Em) spectra of H40-star-mPEG-PhB(OH)$_2$ FNPs. The inset (a) was the visible image of H40-star-mPEG-PhB(OH)$_2$ FNPs in water with the logo of "AIE" as background (left cuvette); the inset was the fluorescent image of H40-star-mPEG-PhB(OH)$_2$ FNPs taken under a UV lamp at 365 nm (right cuvette).

3.2 Biocompatibility of H40-star-mPEG-PhB(OH)$_2$ FNPs

Before FNPs can be potentially used for biomedical applications, it is very important to check their biocompatibility. The preliminary biocompatibility of H40-star-mPEG-PhB$(OH)_2$ FNPs was determined by CCK8 assay. The HeLa cells were incubated with different concentrations (0-120 μg mL^{-1}) of H40-star-mPEG-PhB$(OH)_2$ for both 12 and 24 h. It was worth to noting that neither 12 h nor 24 h interfered with the cell physiology and proliferation within tested concentrations (0-120 μg mL^{-1}). Moreover, even the concentration of H40-star-mPEG-PhB$(OH)_2$ FNPs was up to 120 μg mL^{-1}, the cell viability was closed to 95% (**Fig. 5**). The cell viability results implied that H40-star-mPEG-PhB$(OH)_2$ FNPs had negative adverse effects on cell metabolism and were suitable for cell imaging. In other words, the cytocompatibility of H40-star-mPEG-PhB$(OH)_2$ FNPs will bring another new welfare for cancer therapy and cell imaging.

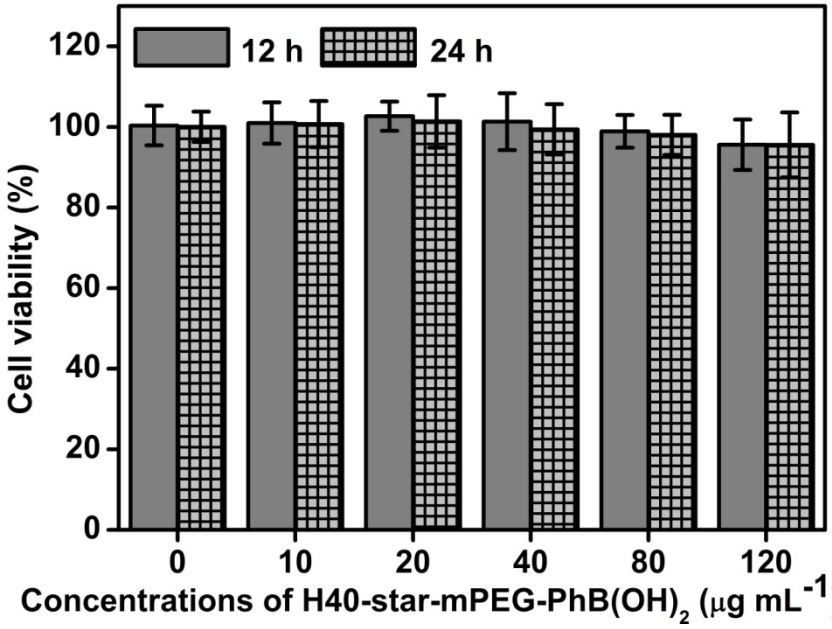

Fig. 5 Biocompatibility evaluation of H40-star-mPEG-PhB$(OH)_2$ FNPs. The cell viability was determined using CCK-8 assay. HeLa cells were incubated with different concentrations of H40-star-mPEG-PhB$(OH)_2$ FNPs for 12 and 24 h.

3.3 Biological imaging of H40-star-mPEG-PhB$(OH)_2$ FNPs

The strong orange-red emission, suitable size and good stability in the water phase of H40-star-mPEG-PhB$(OH)_2$ FNPs prompted us to explore their applications in biological imaging. CLSM for their cell uptake behavior was studied and results were displayed in **Fig. 6**. It could be seen that H40-star-mPEG-PhB$(OH)_2$ FNPs stained HeLa cells effectively and the intensive orange-red fluorescence could be clearly visible, while the intensity in the location of nuclei region was

comparatively weak, which indicated that such H40-star-mPEG-PhB(OH)$_2$ FNPs could readily enter into HeLa cells, while nucleus membrane was impermeable to these luminescent nanoparticles. Besides, thanks to the AIE property, increasing the concentration of H40-star-mPEG-PhB(OH)$_2$ FNPs in staining process could enhance the emission intensity in HeLa cells monotonically without sacrificing the specificity. All the above properties made H40-star-mPEG-PhB(OH)$_2$ FNPs promising for bioimaging applications and drug-loading for cancer treatment.

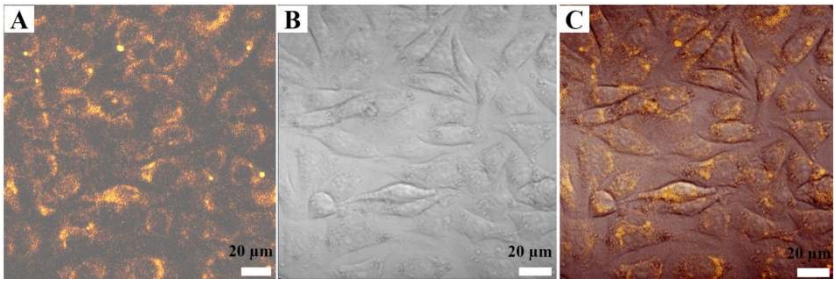

Fig. 6 CLSM imaging of HeLa cells incubated with 40 μg mL^{-1} of H40-star-mPEG-PhB(OH)$_2$ FNPs for 3 h. (A) fluorescent imaging under the excitation with 458 nm laser, (B) bright field, (C) merged image. Scale bar = 20 μm.

4. Conclusions

In summary, a novel type of amphiphilic FNPs based on branched H40, AIE unit (PhB(OH)$_2$) and hydrophilic mPEG unit (mPEG-B(OH)$_2$) have been fabricated through formation of dynamic cyclic borate esters via a facile one-pot strategy. Thus obtained H40-star-mPEG-PhB(OH)$_2$ FNPs were proved to self-assemble in the aqueous solution with uniform spherical morphology, small size, high water dispersibility, strong luminescence, good photostability and low cytotoxicity. Since the hydrophobic H40 as the core, thus bright FNPs with AIE fluorogens offer a new opportunity for biological imaging and drug delivery. Furthermore, this work will open up a new way to development of novel AIE -active FNPs for theranostic applications. Besides, thus one-pot platform for fabrication of AIE-active FNPs in this work will be expected to stimulate new exciting researches and to promote AIE fluorogens as practical tools in biological world in turn.

Acknowledgements

This research was supported by the National Science Foundation of China (Nos. 51363016, 21474057, 21564006, 21561022), and the National 973 Project (Nos. 2011CB935700).

References

[1] W. Qin, D. Ding, J. Liu, W.Z. Yuan, Y. Hu, B. Liu, B.Z. Tang, Biocompatible Nanoparticles with Aggregation‐Induced Emission Characteristics as Far‐Red/Near‐Infrared Fluorescent Bioprobes for In Vitro and In Vivo Imaging Applications, Adv. Funct. Mater., 22 (2012) 771-779.
[2] M. Wang, C.-C. Mi, W.-X. Wang, C.-H. Liu, Y.-F. Wu, Z.-R. Xu, C.-B. Mao, S.-K. Xu, Immunolabeling and NIR-excited fluorescent imaging of HeLa cells by using NaYF4: Yb, Er upconversion nanoparticles, Acs. Nano., 3 (2009) 1580-1586.
[3] S. Zeng, M.-K. Tsang, C.-F. Chan, K.-L. Wong, B. Fei, J. Hao, Dual-modal fluorescent/magnetic bioprobes based on small sized upconversion nanoparticles of amine-functionalized BaGdF 5: Yb/Er, Nanoscale., 4 (2012) 5118-5124.
[4] S. Zeng, M.-K. Tsang, C.-F. Chan, K.-L. Wong, J. Hao, PEG modified BaGdF 5: Yb/Er nanoprobes for multi-modal upconversion fluorescent, in vivo X-ray computed tomography and biomagnetic imaging, Biomaterials., 33 (2012) 9232-9238.
[5] G. Choy, S. O Connor, F.E. Diehn, N. Costouros, H.R. Alexander, P. Choyke, S.K. Libutti, Comparison of noninvasive fluorescent and bioluminescent small animal optical imaging, Biotechniques., 35 (2003) 1022-1031.
[6] T. Ishizawa, N. Fukushima, J. Shibahara, K. Masuda, S. Tamura, T. Aoki, K. Hasegawa, Y. Beck, M. Fukayama, N. Kokudo, Real‐time identification of liver cancers by using indocyanine green fluorescent imaging, Cancer., 115 (2009) 2491-2504.
[7] Y. Yang, S.K. Seidlits, M.M. Adams, V.M. Lynch, C.E. Schmidt, E.V. Anslyn, J.B. Shear, A highly selective low-background fluorescent imaging agent for nitric oxide, J. Am. Chem. Soc., 132 (2010) 13114-13116.
[8] J. Chan, S.C. Dodani, C.J. Chang, Reaction-based small-molecule fluorescent probes for chemoselective bioimaging, Nat. Chem., 4 (2012) 973-984.
[9] M. Fernández-Suárez, A.Y. Ting, Fluorescent probes for super-resolution imaging in living cells, Nat. Rev. Mol. Cell. Bio., 9 (2008) 929-943.
[10] M. Heilemann, S. van de Linde, M. Schüttpelz, R. Kasper, B. Seefeldt, A. Mukherjee, P. Tinnefeld, M. Sauer, Subdiffraction‐resolution fluorescence imaging with conventional fluorescent probes, Angew. Chem. Int. Edit., 47 (2008) 6172-6176.
[11] J. Zhang, R.E. Campbell, A.Y. Ting, R.Y. Tsien, Creating new fluorescent probes for cell biology, Nat. Rev. Mol. Cell. Bio., 3 (2002) 906-918.
[12] S.J. Byrne, S.A. Corr, T.Y. Rakovich, Y.K. Gun'ko, Y.P. Rakovich, J.F. Donegan, S. Mitchell, Y. Volkov, Optimisation of the synthesis and modification of CdTe quantum dots for enhanced live cell imaging, J. Mater. Chem., 16 (2006) 2896-2902.
[13] R. Plass, S. Pelet, J. Krueger, M. Grätzel, U. Bach, Quantum dot sensitization of organic-inorganic hybrid solar cells, J. Phys. Chem. B., 106 (2002) 7578-7580.
[14] L. Turyanska, T.D. Bradshaw, J. Sharpe, M. Li, S. Mann, N.R. Thomas, A. Patane, The Biocompatibility of Apoferritin‐Encapsulated PbS Quantum Dots, Small., 5 (2009) 1738-1741.
[15] J. Weng, X. Song, L. Li, H. Qian, K. Chen, X. Xu, C. Cao, J. Ren, Highly luminescent CdTe quantum dots prepared in aqueous phase as an alternative fluorescent probe for cell imaging, Talanta., 70 (2006) 397-402.
[16] B.-K. An, S.-K. Kwon, S.-D. Jung, S.Y. Park, Enhanced emission and its switching in fluorescent organic nanoparticles, J. Am. Chem. Soc., 124 (2002) 14410-14415.
[17] W.O. McClure, G.M. Edelman, Fluorescent Probes for Conformational States of Proteins. I. Mechanism of Fluorescence of 2-p-Toluidinylnaphthalene-6-sulfonate, a Hydrophobic Probe*,

Biochemistry., 5 (1966) 1908-1919.
[18] T. Terai, T. Nagano, Fluorescent probes for bioimaging applications, Curr. opin. chem. biol, 12 (2008) 515-521.
[19] L. Yuan, W. Lin, K. Zheng, L. He, W. Huang, Far-red to near infrared analyte-responsive fluorescent probes based on organic fluorophore platforms for fluorescence imaging, Chem. Soc. Rev., 42 (2013) 622-661.
[20] Q. Zhao, K. Li, S. Chen, A. Qin, D. Ding, S. Zhang, Y. Liu, B. Liu, J.Z. Sun, B.Z. Tang, Aggregation-induced red-NIR emission organic nanoparticles as effective and photostable fluorescent probes for bioimaging, J. Mater. Chem., 22 (2012) 15128-15135.
[21] J. Luo, Z. Xie, J.W. Lam, L. Cheng, H. Chen, C. Qiu, H.S. Kwok, X. Zhan, Y. Liu, D. Zhu, Aggregation-induced emission of 1-methyl-1, 2, 3, 4, 5-pentaphenylsilole, Chem. Commun., (2001) 1740-1741.
[22] K. Cathy, B. ZhongáTang, Fluorescence enhancements of benzene-cored luminophors by restricted intramolecular rotations: AIE and AIEE effects, Chem. Commun., (2007) 70-72.
[23] Y. Hong, J.W. Lam, B.Z. Tang, Aggregation-induced emission: phenomenon, mechanism and applications, Chem. commun., (2009) 4332-4353.
[24] J. Shi, N. Chang, C. Li, J. Mei, C. Deng, X. Luo, Z. Liu, Z. Bo, Y.Q. Dong, B.Z. Tang, Locking the phenyl rings of tetraphenylethene step by step: understanding the mechanism of aggregation-induced emission, Chem. Commun., 48 (2012) 10675-10677.
[25] N.-W. Tseng, J. Liu, J.C. Ng, J.W. Lam, H.H. Sung, I.D. Williams, B.Z. Tang, Deciphering mechanism of aggregation-induced emission (AIE): Is E–Z isomerisation involved in an AIE process?, Chem. Sci., 3 (2012) 493-497.
[26] X. Zhang, X. Zhang, B. Yang, J. Hui, M. Liu, Z. Chi, S. Liu, J. Xu, Y. Wei, Novel biocompatible cross-linked fluorescent polymeric nanoparticles based on an AIE monomer, J. Mater. Chem. C, 2 (2014) 816-820.
[27] X. Zhang, X. Zhang, B. Yang, J. Hui, M. Liu, W. Liu, Y. Chen, Y. Wei, PEGylation and Cell Imaging Applications of AIE Based Fluorescent Organic Nanoparticles via Ring-opening Reaction, Polym. Chem., 5 (2014) 689-693.
[28] X. Zhang, X. Zhang, B. Yang, L. Liu, J. Hui, M. Liu, Y. Chen, Y. Wei, Aggregation-induced emission dye based luminescent silica nanoparticles: facile preparation, biocompatibility evaluation and cell imaging applications, Rsc. Adv., 4 (2014) 10060-10066.
[29] X. Zhang, X. Zhang, B. Yang, M. Liu, W. Liu, Y. Chen, Y. Wei, Facile fabrication and cell imaging applications of aggregation-induced emission dye-based fluorescent organic nanoparticles, Polym. Chem., 4 (2013) 4317-4321.
[30] X. Zhang, X. Zhang, B. Yang, M. Liu, W. Liu, Y. Chen, Y. Wei, Fabrication of Aggregation Induced Emission Dye-based Fluorescent Organic Nanoparticles via Emulsion Polymerization and Their Cell Imaging Applications, Polym. Chem., 5 (2014) 399-404.
[31] X. Zhang, M. Liu, B. Yang, X. Zhang, Z. Chi, S. Liu, J. Xu, Y. Wei, Cross-linkable Aggregation Induced Emission Dye Based Red Fluorescent Organic Nanoparticles and Their Cell Imaging Applications, Polym. Chem., 4 (2013) 5060-5064.
[32] X. Zhang, X. Zhang, L. Tao, Z. Chi, J. Xu, Y. Wei, Aggregation induced emission-based fluorescent nanoparticles: fabrication methodologies and biomedical applications, Journal of Materials Chemistry B, 2 (2014) 4398-4414.
[33] X. Zhang, X. Zhang, B. Yang, J. Hui, M. Liu, Z. Chi, S. Liu, J. Xu, Y. Wei, Facile Preparation and Cell

Imaging Applications of Fluorescent Organic Nanoparticles that Combine AIE Dye and Ring-opening Polymerization, Polym. Chem., 5 (2014) 318-322.
[34] M. Gao, Q. Hu, G. Feng, B.Z. Tang, B. Liu, A fluorescent light-up probe with "AIE+ ESIPT" characteristics for specific detection of lysosomal esterase, J. Mater. Chem. B., 2 (2014) 3438-3442.
[35] H. Tong, Y. Hong, Y. Dong, M. Häussler, Z. Li, J.W. Lam, Y. Dong, H.H.-Y. Sung, I.D. Williams, B.Z. Tang, Protein detection and quantitation by tetraphenylethene-based fluorescent probes with aggregation-induced emission characteristics, J. Phys. Chem. B, 111 (2007) 11817-11823.
[36] J.-P. Xu, Y. Fang, Z.-G. Song, J. Mei, L. Jia, A.J. Qin, J.Z. Sun, J. Ji, B.Z. Tang, BSA–tetraphenylethene derivative conjugates with aggregation-induced emission properties: Fluorescent probes for label-free and homogeneous detection of protease and α1-antitrypsin, Analyst., 136 (2011) 2315-2321.
[37] Y. Yuan, R.T. Kwok, G. Feng, J. Liang, J. Geng, B.Z. Tang, B. Liu, Rational design of fluorescent light-up probes based on an AIE luminogen for targeted intracellular thiol imaging, Chem. Commun., 50 (2014) 295-297.
[38] Y. Dong, R. Wang, G. Li, C. Chen, Y. Chi, G. Chen, Polyamine-functionalized carbon quantum dots as fluorescent probes for selective and sensitive detection of copper ions, Anal. Chem., 84 (2012) 6220-6224.
[39] H. Lu, B. Xu, Y. Dong, F. Chen, Y. Li, Z. Li, J. He, H. Li, W. Tian, Novel fluorescent pH sensors and a biological probe based on anthracene derivatives with aggregation-induced emission characteristics, Langmuir., 26 (2010) 6838-6844.
[40] M. Wang, G. Zhang, D. Zhang, D. Zhu, B.Z. Tang, Fluorescent bio/chemosensors based on silole and tetraphenylethene luminogens with aggregation-induced emission feature, J. Mater. Chem., 20 (2010) 1858-1867.
[41] Y. Yuan, R.T. Kwok, B.Z. Tang, B. Liu, Targeted Theranostic Platinum (IV) prodrug with a built-in aggregation-induced emission light-up apoptosis sensor for noninvasive early evaluation of its therapeutic responses in situ, J. Am. Chem. Soc., 136 (2014) 2546-2554.
[42] H.-H. Fang, Q.-D. Chen, J. Yang, H. Xia, B.-R. Gao, J. Feng, Y.-G. Ma, H.-B. Sun, Two-photon pumped amplified spontaneous emission from cyano-substituted oligo (p-phenylenevinylene) crystals with aggregation-induced emission enhancement, J. Phys. Chem. C., 114 (2010) 11958-11961.
[43] R. Hu, J.L. Maldonado, M. Rodriguez, C. Deng, C.K. Jim, J.W. Lam, M.M. Yuen, G. Ramos-Ortiz, B.Z. Tang, Luminogenic materials constructed from tetraphenylethene building blocks: Synthesis, aggregation-induced emission, two-photon absorption, light refraction, and explosive detection, J. Mater. Chem., 22 (2012) 232-240.
[44] J. Huang, N. Sun, Y. Dong, R. Tang, P. Lu, P. Cai, Q. Li, D. Ma, J. Qin, Z. Li, Similar or Totally Different: The Control of Conjugation Degree through Minor Structural Modifications, and Deep‐Blue Aggregation‐Induced Emission Luminogens for Non‐Doped OLEDs, Adv. Funct. Mater., 23 (2013) 2329-2337.
[45] Z. Ning, Z. Chen, Q. Zhang, Y. Yan, S. Qian, Y. Cao, H. Tian, Aggregation‐induced Emission (AIE)‐active Starburst Triarylamine Fluorophores as Potential Non‐doped Red Emitters for Organic Light‐emitting Diodes and Cl2 Gas Chemodosimeter, Adv. Funct. Mater., 17 (2007) 3799-3807.
[46] C. Li, X. Liu, S. He, Y. Huang, D. Cui, Synthesis and AIE properties of PEG–PLA–PMPC based triblock amphiphilic biodegradable polymers, Polym. Chem., 7 (2016) 1121-1128.
[47] H. Chen, G. Li, H. Chi, D. Wang, C. Tu, L. Pan, L. Zhu, F. Qiu, F. Guo, X. Zhu, Alendronate-conjugated amphiphilic hyperbranched polymer based on Boltorn H40 and poly (ethylene glycol) for bone-targeted drug delivery, Bioconjugate chem., 23 (2012) 1915-1924.

[48] M. Prabaharan, J.J. Grailer, S. Pilla, D.A. Steeber, S. Gong, Folate-conjugated amphiphilic hyperbranched block copolymers based on Boltorn® H40, poly (l-lactide) and poly (ethylene glycol) for tumor-targeted drug delivery, Biomaterials., 30 (2009) 3009-3019.
[49] C. Tu, L. Zhu, F. Qiu, D. Wang, Y. Su, X. Zhu, D. Yan, Facile PEGylation of Boltorn® H40 for pH-responsive drug carriers, Polymer., 54 (2013) 2020-2027.
[50] S. Aryal, M. Prabaharan, S. Pilla, S. Gong, Biodegradable and biocompatible multi-arm star amphiphilic block copolymer as a carrier for hydrophobic drug delivery, Int. j. biol. macromol., 44 (2009) 346-352.
[51] S. Kim, Y. Shi, J.Y. Kim, K. Park, J.-X. Cheng, Overcoming the barriers in micellar drug delivery: loading efficiency, in vivo stability, and micelle-cell interaction, Expert opin. drug del., 7 (2010) 49-62.
[52] M. Prabaharan, J.J. Grailer, S. Pilla, D.A. Steeber, S. Gong, Amphiphilic multi-arm-block copolymer conjugated with doxorubicin via pH-sensitive hydrazone bond for tumor-targeted drug delivery, Biomaterials., 30 (2009) 5757-5766.
[53] N. Rapoport, Physical stimuli-responsive polymeric micelles for anti-cancer drug delivery, Prog. Polym. Sci., 32 (2007) 962-990.
[54] W. Xu, I.A. Siddiqui, M. Nihal, S. Pilla, K. Rosenthal, H. Mukhtar, S. Gong, Aptamer-conjugated and doxorubicin-loaded unimolecular micelles for targeted therapy of prostate cancer, Biomaterials., 34 (2013) 5244-5253.
[55] X. Yang, J.J. Grailer, S. Pilla, D.A. Steeber, S. Gong, Tumor-targeting, pH-responsive, and stable unimolecular micelles as drug nanocarriers for targeted cancer therapy, Bioconjugate chem., 21 (2010) 496-504.
[56] Y. Zhao, B. Yang, C. Zhu, Y. Zhang, S. Wang, C. Fu, Y. Wei, L. Tao, Introducing mercaptoacetic acid locking imine reaction into polymer chemistry as a green click reaction, Polym. Chem., 5 (2014) 2695-2699.
[57] X. Zhang, X. Zhang, B. Yang, M. Liu, W. Liu, Y. Chen, Y. Wei, Polymerizable Aggregation Induced Emission Dye Based fluorescent Nanoparticles For Cell Imaging Applications Polym. Chem., 5 (2014) 356-360.
[58] H. Wurdak, S. Zhu, K.H. Min, L. Aimone, L.L. Lairson, J. Watson, G. Chopiuk, J. Demas, B. Charette, R. Halder, A small molecule accelerates neuronal differentiation in the adult rat, P. Natl. Acad. Sci., 107 (2010) 16542-16547.
[59] X. Zhang, M. Liu, X. Zhang, F. Deng, C. Zhou, J. Hui, W. Liu, Y. Wei, Interaction of Tannic Acid with Carbon Nanotubes: Enhancement of Dispersibility and Biocompatibility, Toxicol. Res., 4 (2015) 160-168.
[60] X. Zhang, H. Qi, S. Wang, L. Feng, Y. Ji, L. Tao, S. Li, Y. Wei, Cellular responses of aniline oligomers: a preliminary study, Toxicol. Res., 1 (2012) 201-205.
[61] X. Zhang, S. Wang, M. Liu, J. Hui, B. Yang, L. Tao, Y. Wei, Surfactant-dispersed Nanodiamond: Biocompatibility Evaluation and Drug Delivery Applications, Toxicol. Res., 2 (2013) 335-346.
[62] H.S. Abandansari, M.R. Nabid, S.J.T. Rezaei, H. Niknejad, pH-sensitive nanogels based on Boltorn® H40 and poly (vinylpyridine) using mini-emulsion polymerization for delivery of hydrophobic anticancer drugs, Polymer., 55 (2014) 3579-3590.
[63] S. Chen, X.-Z. Zhang, S.-X. Cheng, R.-X. Zhuo, Z.-W. Gu, Functionalized amphiphilic hyperbranched polymers for targeted drug delivery, Biomacromolecules., 9 (2008) 2578-2585.
[64] X. Zeng, W. Tao, Z. Wang, X. Zhang, H. Zhu, Y. Wu, Y. Gao, K. Liu, Y. Jiang, L. Huang, Docetaxel‐Loaded Nanoparticles of Dendritic Amphiphilic Block Copolymer H40‐PLA‐b‐TPGS for Cancer

Treatment, Part. Part. Syst. Char., 32 (2015) 112-122.